Supplement Data:

Supplement Figures

sFigure 1

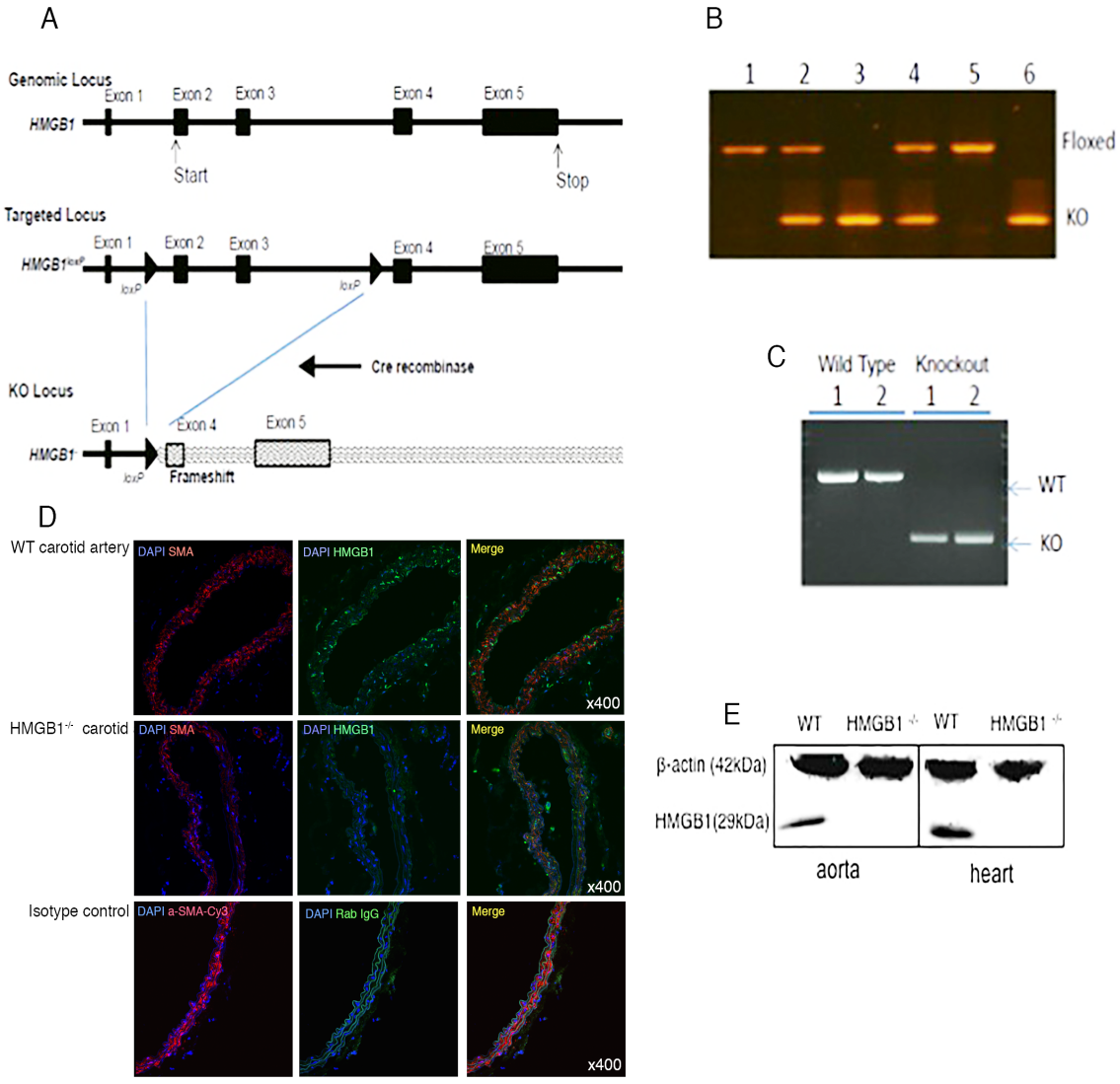

Supplement Figure Legend I.

A: The mouse HMGB1 gene loci for wild type, floxed, and knockout mice are shown. The HMGB1 protein is encoded by four exons and starts from exon 2. Lox/P sequences were placed in introns 1 and 3, therefore Cre-mediated recombination deleted exons 2 and 3, including the initiation codon (ATG). We established the floxed HMGB1 mouse strain to produce a global, inducible HMGB1 knockout mouse. **B:** Genotype analysis of the floxed mice together with heterozygous and knockout mice is shown. **C:** We also measured the RNA expression from the knockout alleles by RT-PCR analysis of the RNA from knockout cells. **D:** Representative sections of uninjured mouse carotid arteries were prepared from WT or HMGB1$^{-/-}$ mice at 35 days after Tamoxifen administration. Immunofluorescence staining was performed to detect HMGB1 expression (green). Nuclei were stained with DAPI (blue). **E:** Tissue lysates from aortic arteries (30μg) were prepared from WT or HMGB1$^{-/-}$ mice at 35 days after tamoxifen and subjected to Western blot analysis with anti-HMGB1 and β-actin antibodies.

sFigure II

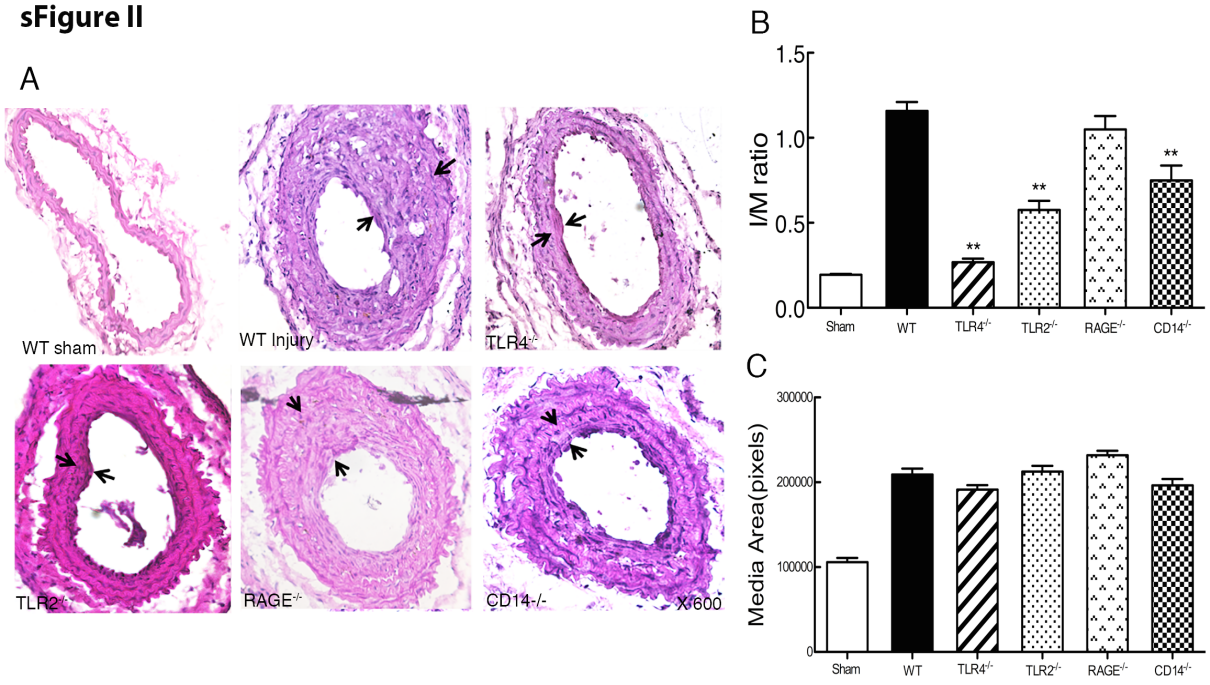

Supplement Figure Legend II.
Intimal hyperplasia in WT, TLR4$^{-/-}$, TLR2$^{-/-}$, RAGE$^{-/-}$, or CD14$^{-/-}$ mice at 28 days following wire injury. A: Representative hematoxylin & eosin (H&E) stained sections of carotid arteries from WT mice (n=10), TLR4 $^{-/-}$ mice (n=10), TLR2 $^{-/-}$ mice (n=6), RAGE $^{-/-}$ mice (n=5), and CD14$^{-/-}$ mice (n=6) are shown. **B-C:** The ratio of intima to media area (I/M) and vessel medial size were quantified by planimetry at 28 days.

sFigure III

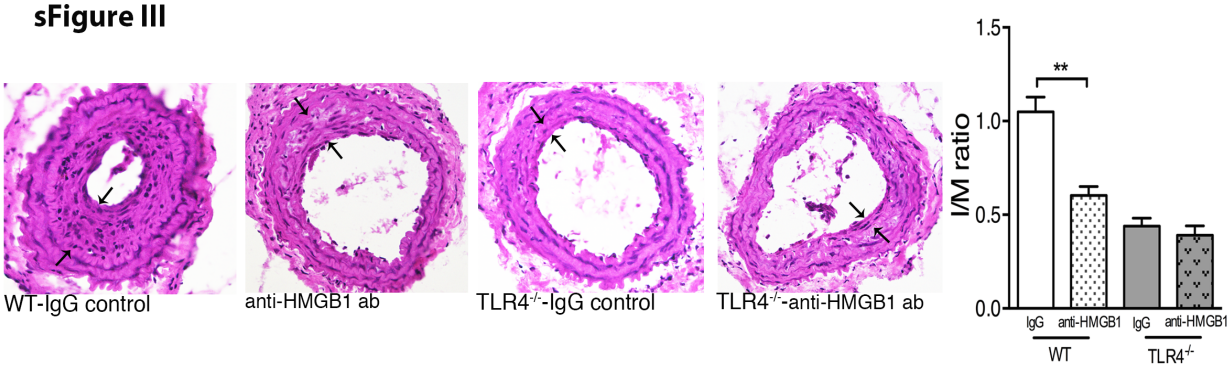

Supplement Figure Legend III.
The anti-HMGB1 neutralizing antibody had no additional effect in reducing IH to TLR4$^{-/-}$ mice due to the deletion of TLR4 results in a marked inhibition of injury-induced intimal hyperplasia. Common carotid arteries were injured by a 0.4-mm guide wire plus external carotid artery ligation and harvested 28 days after surgery. Frozen tissues were sectioned. Representative hematoxylin & eosin (H&E) stained sections of carotid arteries from WT- IgG$_2$b (control antibody) treated mice (n=5), anti-HMGB1 mAb treated mice (n=8), TLR4$^{-/-}$- IgG$_2$b treated mice (n=4) and TLR4$^{-/-}$- anti-HMGB1 mAb treated mice (n=5) are shown. The ratios of intima and media area (I/M) was quantified by planimetry at 28 days. Representative hematoxylin & eosin (H&E) stained sections are shown. Data represent the means ± SEM. **P<0.01 versus the indicated groups.

sFigure IV

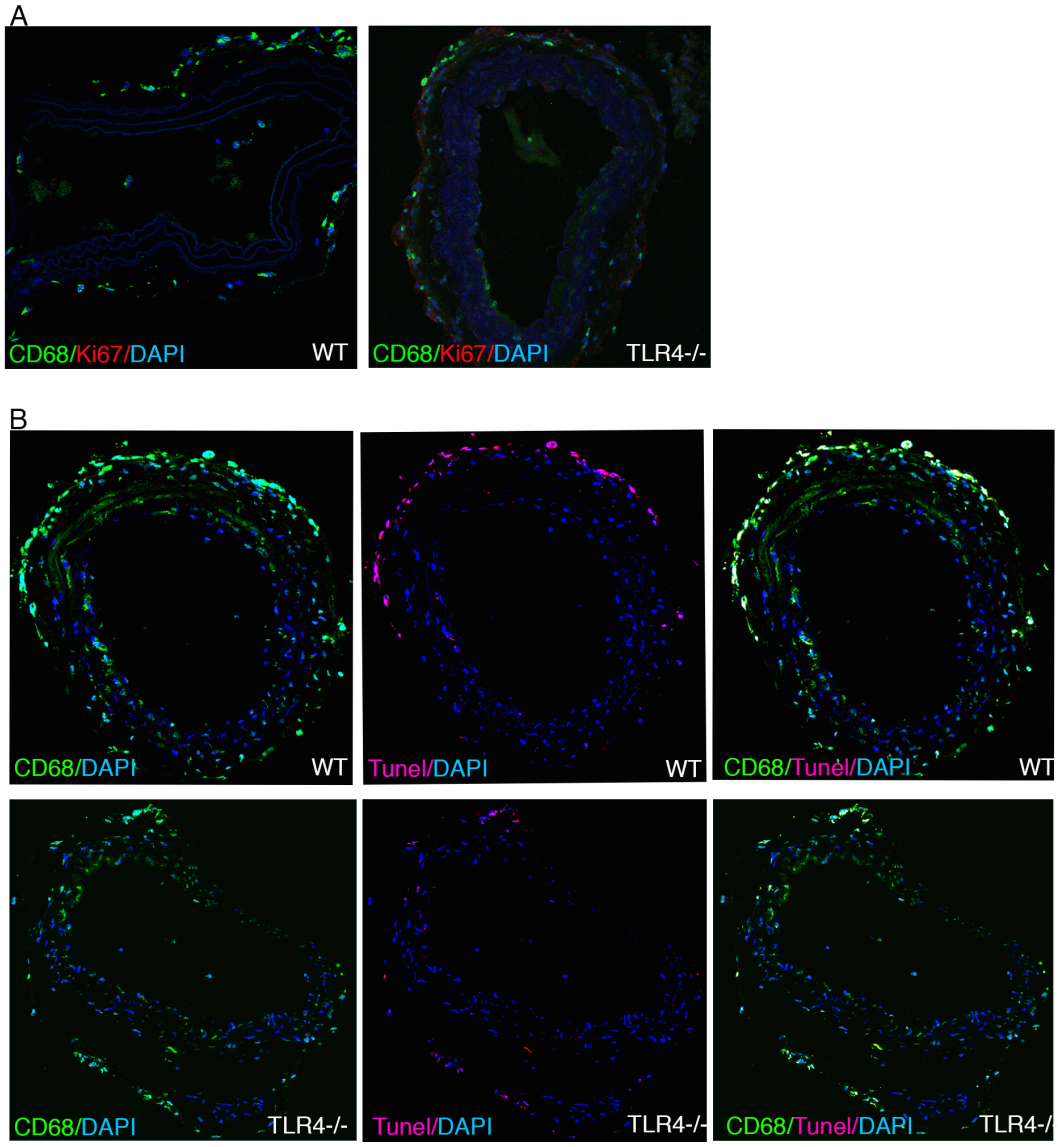

Supplement Figure Legend IV.
No Ki67+CD68+ cells in the injured arteries of either WT or TLR4$^{-/-}$ mice at 3 days. TUNEL+ cells were lower in the TLR4$^{-/-}$ mice compared to WT mice at 3 days.
A: Immunofluorescence staining was performed to detect CD68 expression (green) co-localized with proliferating cells (Ki67, red) in carotid arteries from WT mice at 3 days. Ki67 positive- cells were not observed in the injured arteries of either WT or TLR4$^{-/-}$ mice at 3 days **B:** Dapi (blue), CD68 (green) and TUNEL (red) triple positive (white) cells were reduced in TLR4 $^{-/-}$ mice compared to WT mice at 3 days post arterial injury. Representative fluorescent–stained sections are shown.

sFigure V

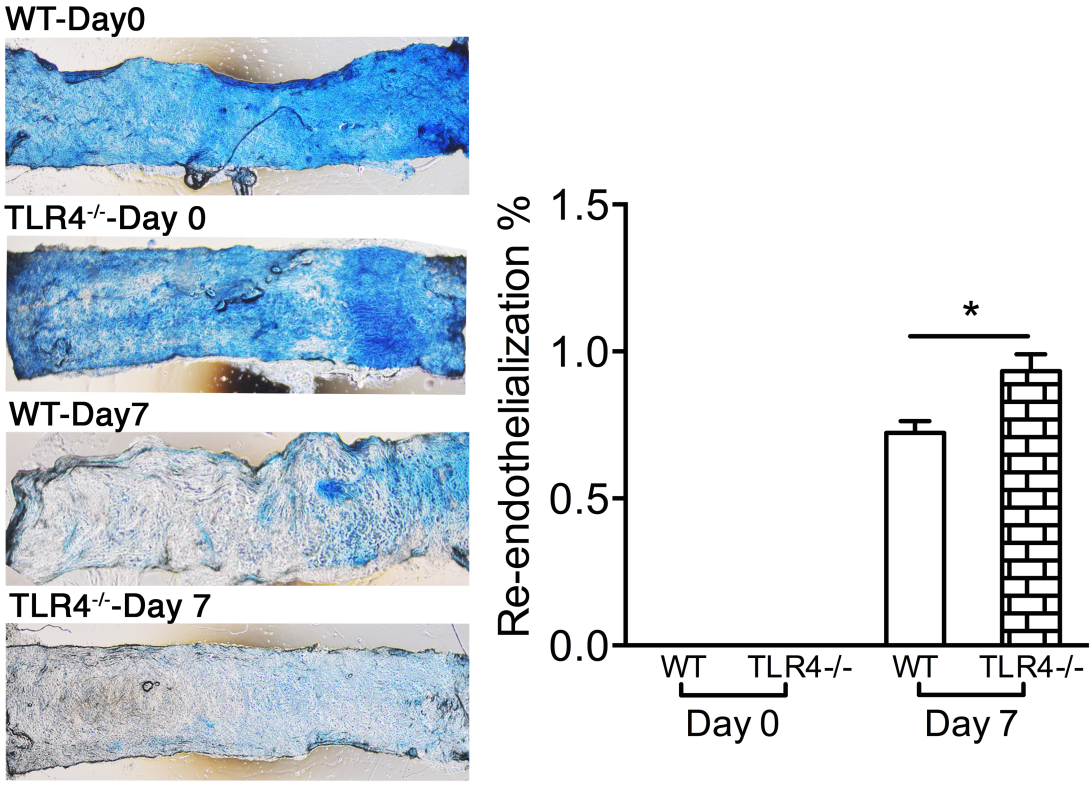

Supplement Figure Legend V.
Faster re-endothelialization in the TLR4$^{-/-}$ strain compared to the WT mice. Re-endothelialization of the carotid artery following endothelium denudation. Complete removal of endothelium was verified with Evans blue staining in vivo immediately after carotid injury (Day0); Re-endothelialization was quantified by Evans blue staining at Day 7 following injury and is expressed as a percentage of non-stained area to the total en face area of the carotid artery (n = 3 in each group).

sFigure VI

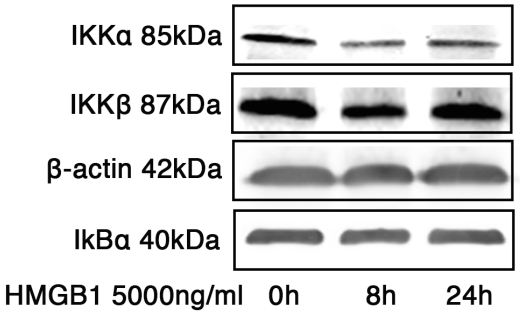

Supplement Table I: Origins of mutant mice

Strain	Acronym	Origin
C57BL/6 wild-type mice	WT	Jackson Laboratory
HMGB1 loxP/loxP[1]	HMGB1 $^{loxP/loxP}$	Dr. Timothy Billiar (Department of Surgery, University of Pittsburgh School of Medicine, Pittsburgh, PA)
HMGB1 knockout mice	HMGB1 $^{-/-}$	Dr. Qingde Wang (Department of Surgery, University of Pittsburgh School of Medicine, Pittsburgh, PA)
TLR4 knockout mice[2]	TLR4$^{-/-}$	Dr. Timothy Billiar (Department of Surgery, University of Pittsburgh School of Medicine, Pittsburgh, PA)
TLR4 loxP/loxP[2]	TLR4 $^{loxP/loxP}$	Dr. Timothy Billiar (Department of Surgery, University of Pittsburgh School of Medicine, Pittsburgh, PA)
TLR2 knockout mice[3]	TLR2$^{-/-}$	Dr. Shizuo Akira (Research Institute for Microbial Diseases, Osaka University, Osaka, Japan)
RAGE knockout mice[4]	RAGE$^{-/-}$	Dr. Timothy Billiar (Department of Surgery, University of Pittsburgh School of Medicine, Pittsburgh, PA)
Trif mutant mice[5]	TRIF^{LPS2}	Dr. Bruce Beutler (University of Texas Southwestern Medical Center, Dallas, TX)
MyD88 competent mice[6]	MyD88$^{+/+}$	Dr. Ruslan Medhzitov (Howard Hughes Medical Institute, Yale School of Medicine, New Haven, CT)
MyD88 knockout mice[6]	MyD88$^{-/-}$	Dr. Ruslan Medhzitov (Howard Hughes Medical Institute, Yale School of Medicine, New Haven, CT)
Myeloid cell TLR4 knockout mice (macrophages, granulocytes, and monocytes)[7]	Lyz-TLR4$^{-/-}$	Dr. Timothy Billiar (Department of Surgery, University of Pittsburgh School of Medicine, Pittsburgh, PA)
CD14 knockout mice[8]	CD14$^{-/-}$	Dr. Mason Freeman (Massachusetts General Hospital, Harvard Medical School, Boston, MA)

Supplement Table II: PCR primers

	Forward	Reverse
mTLR4	CTCTGCCTTCACTACAGAGAC	TGGATGATGTTGGCAGCAATG
mTLR2	GTTCTCCCAGCATTTAAAATCATT	GTCTCCAGTTTGGGAAAAGAACC
mMyD88	GGCAACTAGAACAGACAGAC	CAAATGCTGAAACTATAGG
mTrif	CACAGTCCCAATCCTTTC	TCACTCTGGAGTCTCAAG
mIL-6	CACAGAGGATACCACTCCCAACA	TCCACGATTTCCCAGAGAACA
mIFN-β	AGCTCCAAGAAAGGACGAACA T	GCCCTGTAGGTGAGGTTGATC T
mCD14	CGCGGATTCCTAGTCGG	CGCAGGAAAAGTTGAGTGAGT
mMD2	CTCCGATGCAATTATTTCCTAC	TGGCACAGAACTTCCTTACG
mMCP-1	TCACCTGCTGCTACTCATTCACCA	AAAGGTGCTGAAGACCCTAGGGCA
mCCR2	CCTGCAAAGACCAGAAGAGG	GTGAGCAGGAAGAGCAGGTC
mPDGF-A	CCTGTGCCCATCCGCAGGAAGAGA	TTGGCCACCTTGACGCTGCGGTG
m18S	CGGCTACCACATCCAAGGAA	GCTGGAATTACCGCGGCT

References:

1. Kang R, Zhang Q, Hou W, et al. Intracellular hmgb1 inhibits inflammatory nucleosome release and limits acute pancreatitis in mice. *Gastroenterology*. 2014;146:1097-1107
2. Ding N, Chen G, Hoffman R, Loughran PA, Sodhi CP, Hackam DJ, Billiar TR, Neal MD. Toll-like receptor 4 regulates platelet function and contributes to coagulation abnormality and organ injury in hemorrhagic shock and resuscitation. *Circulation. Cardiovascular genetics*. 2014;7:615-624
3. Kim HS, Go H, Akira S, Chung DH. Tlr2-mediated production of il-27 and chemokines by respiratory epithelial cells promotes bleomycin-induced pulmonary fibrosis in mice. *J Immunol*. 2011;187:4007-4017
4. Raman KG, Sappington PL, Yang R, Levy RM, Prince JM, Liu S, Watkins SK, Schmidt AM, Billiar TR, Fink MP. The role of rage in the pathogenesis of intestinal barrier dysfunction after hemorrhagic shock. *American journal of physiology. Gastrointestinal and liver physiology*. 2006;291:G556-565
5. Tabeta K, Georgel P, Janssen E, Du X, Hoebe K, Crozat K, Mudd S, Shamel L, Sovath S, Goode J, Alexopoulou L, Flavell RA, Beutler B. Toll-like receptors 9 and 3 as essential components of innate immune defense against mouse cytomegalovirus infection. *Proceedings of the National Academy of Sciences of the United States of America*. 2004;101:3516-3521
6. Jiang D, Liang J, Fan J, et al. Regulation of lung injury and repair by toll-like receptors and hyaluronan. *Nature medicine*. 2005;11:1173-1179
7. Chyu KY, Dimayuga P, Zhu J, Nilsson J, Kaul S, Shah PK, Cercek B. Decreased neointimal thickening after arterial wall injury in inducible nitric oxide synthase knockout mice. *Circulation research*. 1999;85:1192-1198
8. Jeyaseelan S, Chu HW, Young SK, Freeman MW, Worthen GS. Distinct roles of pattern recognition receptors cd14 and toll-like receptor 4 in acute lung injury. *Infection and immunity*. 2005;73:1754-1763

Materials and Methods

Antibodies against CD68 (ab125212), MCP-1/CCL2 (ab21396), CCR2 (ab21667), and HMGB1 (ab18256) were obtained from Abcam. MD2 (NBP1-77201) from Novus biological. MYD88 (SAB2500664), β-actin (A1978), Anti-Actin, and α-Smooth Muscle - Cy3 (C6198) were purchased from Sigma. HMGB1 (sc-12523), TLR4 (sc-8694, sc-30002) and NFκB P65 (sc-71677) were obtained from Santa Cruz Biotechnology. pIKK α/β (2078P), pIκBα (2859P), and Ki67 (9129S) were obtained from Cell Signaling. HMGB1 ELISA kit was purchased from IBL International. Mouse TNF-alpha Quantikine ELISA Kit (MTA00B), Human/Mouse PDGF-AA Quantikine ELISA Kit (DAA00B) and Mouse IL-6 Quantikine ELISA Kit (M6000B) were obtained from R&D Systems.

TLR4-inhibitory peptide (Viper) and control peptide (CP-7) were obtained from Imgenex (San Diego, CA). Monoclonal antibody against HMGB1 (2G7) [1], nonimmune mouse IgG_2b, disulfide HMGB1 [2], a tetramer P5779[3] and scrambled control peptide (provided by Dr. Kevin Tracey, Feinstein Institute for Medical Research) were prepared as described previously. The neutralizing activity of anti-HMGB1 mAb has been confirmed in cell culture assays as well as animal models of HMGB1-mediated damage [4, 5]. In the in vivo study, mice were given anti-HMGB1 mAb intraperitoneally (50μg/mice) once a day at two days before surgery and daily post-surgery. Mice received intraperitoneal injection of P5779 (500 μg/mouse) or vehicle twice a day post-surgery. Disulfide HMGB1 refers to HMGB1 with cysteine 23 and 45 disulfide bonded and cysteine 106 in the thiol configuration.

Animals

TLR4 $^{loxP/loxP}$ and cell-specific TLR4$^{-/-}$ mice were generated as described previously [6]. To prevent neonatal death of mice with MyD88 adaptor protein loss-of-function, MyD88$^{+/+}$ and MyD88$^{-/-}$ mice were bred as described previously [7]. All mutant strains were backcrossed at least 10 times into a C57BL/6 background and used at the age of 8-12 weeks. Animals were maintained on a 12 hour light-dark cycle in a pathogen-free facility at the University of Pittsburgh (Pittsburgh, PA) and were fed a standard diet with water. The experimental design was approved by the University of Pittsburgh Institutional Animal Care and Use Committee. The origins of all mutant mice used are listed in the Online Data Supplement Table 1.

Generation of Inducible Global HMGB1$^{-/-}$ Mice

The floxed HMGB1 mouse was generated as previously described [8]. The targeted allele was designed to have two Lox/P elements inserted into introns 1 and 3. The flanking region of the two Lox/P elements includes exon 2 in which incudes the transcription initiation codon covers most of the HMGB1 coding region. Before generating the chimeric mouse with the correct ES cell clones, the selection marker, Neo gene cassette, was removed by *in vitro* FRP recombination. Therefore only two short Lox/P elements remained in the mouse genome. We confirmed that this modification of the genome did not affect HMGB1 gene expression [8]. sFigure 1 illustrates the HMGB1 allele in wild type, floxed, and knockout cells and shows the analysis of the floxed and knockout mice.

Global inducible HMGB1 knockout mice were generated because embryonic deletion was shown to be lethal shortly after birth [9], preventing the *in vivo* functional study of the HMGB1 gene beyond this very early age. The strain used in this study was generated by introducing the inducible Cre transgene into HMGB1 floxed mice. The transgene is driven by a ubiquitously active CAG promoter and expresses a Cre and estrogen receptor fusion protein. This fusion protein changes its configuration upon binding to estrogen or estrogen analog such as tamoxifen (TM) and translocates into the cell nucleus to excise the floxed gene. We confirmed that HMGB1 expression was intact

in the inducible knockout mouse until TM was administered to the animal by intraperitoneal injection. ***Tamoxifen was administered to the animals by intraperitoneal injection 7 days before the carotid artery injury procedure.*** Although HMGB1 deletion in very young mice (less than three weeks old) leads to death, deletion in young adults mice (6 weeks of age or older) was well tolerated.

Carotid Artery Injury Model

Carotid artery wire injury was induced just proximal to the carotid bifurcation previously described [10]. Briefly, mice were anesthetized with isoflurane. The left carotid artery was exposed on the ventral side of the neck via a midline incision. The bifurcation of the right carotid artery was located, and two ligatures (surgical silk, size 6-0, Deknatel, Queens Village, NY) were placed around the external carotid artery, which was then tied off with the distal ligature. After temporarily occlusion of the internal carotid artery, a small incision was made between the two ligatures placed around the external carotid artery, and a curved, *0.014-inch (= 0.38 mm) guide wire* (C-SF-15-15, Cook Belgium, NV) was passed toward the aortic arch and withdrawn three times with a rotating motion to denude endothelial cells. Ligation of the external carotid artery was applied after withdrawal of the guide wire to increase the neointimal area [11]. The skin incision was closed with a single suture. Animals were allowed to recover and carotid arteries were harvested 28 days after the injury.

Lentiviral Transduction of the Carotid Artery Injury *in situ*

Before wound closure, 100µl 20% pluronic gel (Sigma Aldrich, The Netherlands) containing 1×10^6 lentiviral particles (sc-35987-V, Santa Cruz Biotechnology, Texas, USA) was applied around the carotid artery along with 0.8µg/ml DEAE (Sigma Aldrich, The Netherlands) for lubrication.

Histological and Morphometric Analysis

Carotid arteries were harvested at the indicated times after injury. Five to six 6µm-thick sections, cut 100 µm apart from each other, were stained with hematoxylin and eosin-stained. The five-six sections obtained from each arterial segment were analyzed by using computerized morphometry (ImageJ software, National Institutes of Health), and the average values were calculated. Measurements included luminal area, medial area, intimal area, vessel area, and the lengths of the internal elastic lamina and external elastic lamina. The intima-to-media (I/M) ratio was calculated as previously described. All sections were analyzed separately by two investigators blinded to the study design. Immunohistochemical analyses were processed according to standard procedures.

Immunofluorescent Staining

Carotid arteries were harvested at the indicated times after injury and were fixed in 2% paraformaldehyde for two hours. Tissue was placed in 30% sucrose for 24 hours. 6µm cryostat sections were obtained and put onto gelatin-coated glass slides. 0.1% Triton X-100 was permeabilized for 10 minutes and blocked with 2% bovine serum albumin for 45 minutes. Tissues were then incubated in primary antibodies over night at 4°C followed by incubation for 60 minutes with fluorescent-labeled secondary antibodies. After nuclear staining for 30 seconds with DAPI, slides were covered using Gelvatol. Antibody dilutions were prepared as follows: HMGB1, 1:100; TLR4, 1:100; CCR2, 1:100; CD68, 1:100; Ki67, 1:100; SMA, 1:1000; MyD88, 1:200; secondary donkey anti-Goat (Cy3) and donkey anti-rabbit (488) Alexa Fluor–conjugated antibodies, 1:500; Anti-Actin, and α-Smooth Muscle - Cy3, 1:1000 and 4', 6-diamidino-2-phenylindole (DAPI), 1:2000. Images were taken using an Olympus Provis Fluorescence Microscope or an Olympus Fluoview 500

confocal microscope at the University of Pittsburgh Center for Biologic Imaging. Quantitative analyses of immuhistochemistry experiments were performed on digitized images (10xprimary magnification) by using the Photoshop software. The presentative sections at the level of the injured carotid artery were taken from each animal (3-5 animals per genotype). To count CD68-positive cells in the carotid artery, four squared counting boxes (75μm per side) were taken per section. To count HMGB1-and Ki67 positive cells in the carotid artery, four squared counting boxes (100μm per side) were taken per section. The carotid arteries cross-sectional slides were counted blindly by 2 independent observers.

Cell Culture

Human aortic smooth muscle cells (HASMC) were obtained from Cell Applications, Inc. (San Diego, CA) and were cultured in DMEM/F12 (Lonza Walkersville, Inc) with 20% FBS. Prior to each experiment, cells were serum-starved overnight in basal medium. Cells were used between passages 4 and 9.

THP-1 monocytic cells (0.5×10^6 cells/ml) were differentiated into macrophages in 60 mm dishes containing 2 ml RPMI 1640 medium containing 10ng/ml phorbol 12-myristate 13-acetate (PMA) over 48 hours. For disulfide HMGB1 treatments, macrophages differentiated with 10 ng/ml PMA were washed with phosphate buffered saline (PBS) and incubated in 1ml of serum free RPMI 1640 for three hours. The macrophages were then treated with 5ug/ml of disulfide HMGB1 for eight hours. The supernatants were collected after culturing for eight hours and stored at –80 °C until needed for cytokine analysis.

Thioglycollate-elicited murine peritoneal macrophages were harvested by lavage from $TLR4^{-/-}$, $TLR2^{-/-}$, $Trif^{Lps2}$, $MyD88^{-/-}$, and $CD14^{-/-}$ mice and matched with WT mice. Peritoneal macrophages were cultured in RPMI 1640 (Hyclone@ Thermo Scientific) supplemented with 10% fetal bovine serum (Sigma-Aldrich). After three hours of adherence, cells were washed twice and treated with agent for eight hours.

Migration Assay

HASMC were seeded onto six-well plates. Cells were grown to confluence, serum-starved overnight, and treated with disulfide HMGB1 (1 or 5μg/ml) alone or in combination with TLR4-inhibitory peptide (Viper 30μM) or control peptide (CP-7 30μM). The monolayer of cells was scratched by a 200μL sterile pipette tip. Images were obtained at three and six hours after treatment. Wound area was determined using ImageJ software (National Institutes of Health) and migration was calculated as a percentage of decrease in wound area.

A quantitative SMC migration assay was performed using a BD BioCoat Cell Migration FluoroBlok 96-multiwell insert system (BD Biosciences, Cat. No. 351164). The insert contained a fluorescence-blocking, 8-μm pore size PET membrane coated with a BD Matrigel matrix that serves as a reconstituted authentic basement membrane. The 8-μm pore allows epithelial cells, fibroblasts, tumor cells, smooth muscle cells and osteoblasts go throught PET membrane. The passage of cells through the BD FluoroBlok membrane was measured. *Allow SMC migrate for 20 hours.* To do this insert was transferred to a second plate containing the calcein AM solution and incubated for 90 minutes. The FluoroBlok 96-well insert system allowed quantification of the number of cells that migrated or invaded through the pores by a bottom-reading fluorometer at excitation/emission wavelengths of 494/517 nm.

Cell Proliferation Assay

For the determination of viable cell number, HASMC were plated in 96-well plates at a density of approximately 3,000 cells/well in the experimental medium. Eight hours after

plating, cells were treated with various agents as indicated in each experiment. The number of viable cells was determined using a CellTiter Aqueous One Solution Cell Proliferation Assay Kit from Promega (Madison, WI) according to the manufacturer's instruction.

Reverse Transcription-Quantitative PCR

RNA from carotid artery tissue was isolated using the RNeasy Mini Kit (Qiagen). Reverse-transcription into cDNA and quantitative PCRs were carried out using iScript™ One-Step RT-PCR Kit With SYBR® Green (Bio-Rad, Hercules, CA). The reaction was run on a CFX96™ Real-time PCR detection system.

PCR primers listed in the Online Supplement Table 2 were used as an internal control and the data are expressed as fold of a corresponding control.

Western Blot Analysis

Whole cell lysates were collected in CelLytic™ MT Cell Lysis Reagent (Sigma Aldrich) and protease inhibitor cocktail (Sigma Aldrich). Whole cell lysates were collected and protein concentrations determined by the micro bicinchoninic acid assay (Pierce). Equal amounts of lysates (30 μg protein) were separated by SDS-PAGE and transferred to a nitrocellulose membrane that was blocked with Odyssey blocking buffer (LI-COR, Lincoln, NE) for 60 minutes, followed by incubation overnight at 4°C with an anti-β actin (1:2000), anti-MCP-1/CCL2 (1:1000), anti-CCR2 (1:1000), pIKK α/β(1:500), pIκBα(1:1000) antibody, and then washed before incubation with species-appropriate, fluorescently conjugated secondary antibodies for one hour at room temperature. Membranes were analyzed using an Odyssey Infrared Imaging System (LI-COR; Millennium Science, Surrey Hills, Australia) and relevant signal intensity was determined using ImageJ software (National Institutes of Health). Significance was examined using Student's t test; a p value of <0.05 was considered significant.

Serum or cell medium analysis

Blood samples were obtained from animals via cardiac puncture at various time points post-surgery. Cell supernatants were collected after eight-hour treatment with disulfide HMGB1. Serum or cell supernatants were collected and stored at -80 °C until analysis was performed. HMGB1, TNF-α, IL-6, MCP-1/CCL2 and PDGF-A levels were measured using enzyme-linked immunosorbent assays (ELISAs) performed according to the manufacturer's instructions.

Preparation of HMGB1-treated Macrophage Conditioned Media(CM)

THP-1 monocytic cells (0.5×10^6 cells/ml) were differentiated into macrophages in 60 mm dishes containing 2 ml RPMI 1640 medium containing 10ng/ml PMA over 48 hours. The supernatants were then collected in 15 ml tubes and the plates were washed three times with 5 ml PBS and combined with the supernatant. For the disulfide HMGB1 treatments, the macrophages differentiated with 10ng/ml PMA were washed with PBS and incubated in 2 ml of serum free RPMI 1640 for two hours. The macrophages were then treated with 5000ng/ml disulfide HMGB1 for eight hours. The supernatants were collected and place on cultured HASMC culturing or stored at –80 °C until ready for use.

References:

1. Schierbeck H, Lundback P, Palmblad K, Klevenvall L, Erlandsson-Harris H, Andersson U, Ottosson L. Monoclonal anti-hmgb1 (high mobility group box

chromosomal protein 1) antibody protection in two experimental arthritis models. *Mol Med*. 2011;17:1039-1044
2. Yang H, Lundback P, Ottosson L, Erlandsson-Harris H, Venereau E, Bianchi ME, Al-Abed Y, Andersson U, Tracey KJ, Antoine DJ. Redox modification of cysteine residues regulates the cytokine activity of high mobility group box-1 (hmgb1). *Mol Med*. 2012;18:250-259
3. Yang H, Wang H, Ju Z, Ragab AA, Lundback P, Long W, Valdes-Ferrer SI, He M, Pribis JP, Li J, Lu B, Gero D, Szabo C, Antoine DJ, Harris HE, Golenbock DT, Meng J, Roth J, Chavan SS, Andersson U, Billiar TR, Tracey KJ, Al-Abed Y. Md-2 is required for disulfide hmgb1-dependent tlr4 signaling. *The Journal of experimental medicine*. 2015;212:5-14
4. Yang H, Ochani M, Li J, Qiang X, Tanovic M, Harris HE, Susarla SM, Ulloa L, Wang H, DiRaimo R, Czura CJ, Wang H, Roth J, Warren HS, Fink MP, Fenton MJ, Andersson U, Tracey KJ. Reversing established sepsis with antagonists of endogenous high-mobility group box 1. *Proceedings of the National Academy of Sciences of the United States of America*. 2004;101:296-301
5. Qin S, Wang H, Yuan R, Li H, Ochani M, Ochani K, Rosas-Ballina M, Czura CJ, Huston JM, Miller E, Lin X, Sherry B, Kumar A, Larosa G, Newman W, Tracey KJ, Yang H. Role of hmgb1 in apoptosis-mediated sepsis lethality. *The Journal of experimental medicine*. 2006;203:1637-1642
6. Nace GW, Huang H, Klune JR, Eid RE, Rosborough BR, Korff S, Li S, Shapiro RA, Stolz DB, Sodhi CP, Hackam DJ, Geller DA, Billiar TR, Tsung A. Cellular specific role of toll-like receptor 4 in hepatic ischemia-reperfusion injury. *Hepatology*. 2013
7. Buchholz BM, Billiar TR, Bauer AJ. Dominant role of the myd88-dependent signaling pathway in mediating early endotoxin-induced murine ileus. *American journal of physiology. Gastrointestinal and liver physiology*. 2010;299:G531-538
8. Huang H, Nace GW, McDonald KA, Tai S, Klune JR, Rosborough BR, Ding Q, Loughran P, Zhu X, Beer-Stolz D, Chang EB, Billiar T, Tsung A. Hepatocyte specific hmgb1 deletion worsens the injury in liver ischemia/reperfusion: A role for intracellular hmgb1 in cellular protection. *Hepatology*. 2013
9. Calogero S, Grassi F, Aguzzi A, Voigtlander T, Ferrier P, Ferrari S, Bianchi ME. The lack of chromosomal protein hmg1 does not disrupt cell growth but causes lethal hypoglycaemia in newborn mice. *Nature genetics*. 1999;22:276-280
10. Kumar A, Lindner V. Remodeling with neointima formation in the mouse carotid artery after cessation of blood flow. *Arteriosclerosis, thrombosis, and vascular biology*. 1997;17:2238-2244
11. Yu P, Nguyen BT, Tao M, Campagna C, Ozaki CK. Rationale and practical techniques for mouse models of early vein graft adaptations. *Journal of vascular surgery*. 2010;52:444-452